Imaging a Polygonal Network of Ice-Wedge Casts with an Electromagnetic Induction Sensor

Eef Meerschman*
Marc Van Meirvenne
Philippe De Smedt
Timothy Saey
Mohammad Monirul Islam
Fun Meeuws
Ellen Van De Vijver
Gunther Ghysels
Res. Group Soil Spatial Inventory Techniques
Dep. of Soil Management
Faculty of Bioscience Engineering
Ghent Univ.
Coupure 653
9000 Gent, Belgium

Images of the morphology of a polygonal network of ice-wedge casts are a valuable aid to paleoclimatological reconstructions. Usually such images are obtained by aerial photography showing polygonal crop marks reflecting textural differences between wedge filling and host material. Our objective was to investigate an alternative method by measuring the soil apparent electrical conductivity (EC_a) with an electromagnetic induction (EMI) sensor. Based on an aerial photograph showing polygonal crop marks in an agricultural field in Belgium, a test area of 0.63 ha was selected. A small part of the test area (6 by 6 m) was excavated revealing a clear pattern of ice-wedge casts. The wedges penetrated clay-rich Tertiary marine sediments, covered by a 0.6-m layer of eolian sandy sediments, and were associated with the permafrost during the last glacial period. We took 94 subsoil (0.6–0.8 m) samples distributed over the test area and analyzed their texture. The results showed a clear difference between the Eocene host material (on average 21% clay) and the Quaternary wedge filling (on average 6% clay). The test area was surveyed with an EMI sensor (we used an EM38DD) which resulted in an accurate image of the polygonal network. We concluded that an EMI survey is an appropriate technique to image the morphology of a polygonal network of subsoil ice-wedge casts. A final perspective comprises the strong heterogeneity of the subsoil, since nearly half of the subsoil consists of ice-wedge material. This might open perspectives for precision agriculture in such landscapes.

Abbreviations: DOE, depth of exploration; EC_a, apparent electrical conductivity; EMI, electromagnetic induction.

In many parts of the mid-latitudes of the northern hemisphere, the past existence of peri-glacial conditions is evidenced by the presence of ice-wedge casts and relic sand wedges (French, 2007). These cryogenic structures are the remnants of thermal contraction cracks formed in permafrost-affected soils (Kolstrup, 1986). Progressive infilling of these cracks with ice, sand or both, resulted in wedge-shaped bodies of ice, sand or sand-ice (French, 2007; Ghysels and Heyse, 2006; Murton and French, 1993; Vandenberghe and Pissart, 1993). When changing climatic conditions caused the permafrost to thaw, the wedge-shaped cavities were filled with wind- and water-transported sediments resulting in their preservation as ice-wedge casts or ice-wedge pseudomorphs (Harry and Gozdzik, 1988). Consequently, the wedge filling has a different composition than the host material.

The surface expression of thermal contraction cracks is generally a network of polygons, still observable in modern periglacial environments at high latitudes (French, 2007). In central Europe and North America, polygonal networks of ice-wedge casts were often covered by eolian or fluviatile loess or sand, so their pattern is rarely directly observable. However, the morphology of these polygonal networks provides valuable information about past environmental and climatic conditions, since their formation depend on many factors such as soil temperature gradients, mineral composition of the soil, moisture content and variations in air temperature (Dutilleul et al., 2009; Mackay and Burn, 2002; Plug and Werner, 2002, 2008; Romanovskij, 1973). Apart from imaging the ice-wedge casts for paleoclimatological reconstructions, characterizing their abrupt chang-

Soil Sci. Soc. Am. J. 75:2011
Posted online 8 Sept. 2011
doi:10.2136/sssaj2011.0063
Received 17 Feb. 2011.
*Corresponding author (eef.meerschman@ugent.be).

es in soil composition can suit other purposes. Ice-wedge casts can have an impact on engineering projects (Morgan, 1971), preferential flow paths for leaching to groundwater (Dansart et al., 1999), and on crop yield calling for techniques known as precision agriculture.

Occasionally, near-surface networks of pseudomorphs show up on aerial photographs of cultivated fields due to color contrasts of the crop, called crop marks. These are caused by pedological differences between host material and wedge filling. However, the occurrence of crop marks is very sensitive to variations in soil type, soil moisture content, vegetation type, nutrient availability, and meteorological conditions (Walters, 1994). Therefore, the time frame for such observations is often very narrow and the costs of obtaining them are large. In the particular situations where crop marks reveal the presence of ice-wedge casts, aerial photographs can be used to map the polygonal network morphology (Ghysels, 2008; Lusch et al., 2009).

Near-surface geophysical prospection methods are an alternative for mapping polygonal networks of ice-wedge casts. A few studies have shown the use of ground-penetrating radar (Dansart et al., 1999; Doolittle and Nelson, 2009) and electrical resistivity (Lusch et al., 2009) to detect relic ice-wedges. Cockx et al. (2006) were the first to map near-surface Pleistocene ice-wedge casts with an electromagnetic induction (EMI) sensor. However, their survey covered a small excavated area where the casts were visible at the surface.

The aim of this study is to assess the potential of an EMI soil sensor to image subsurface ice-wedge casts in an agricultural field. We selected an area in Belgium based on an available aerial photograph showing polygonal crop marks.

MATERIALS AND METHODS

Aerial Photograph and Test Area

Figure 1a shows a part of an oblique aerial photograph of an agricultural field in Deinze, Belgium (central coordinates: 51°01′16″ N, 3°29′41″ E). The field is situated on the West Flanders plateau, a low-lying plateau (25 m above sea level) between the Coastal Plain and the Flemish Valley.

The photograph was taken on 4 Aug. 1996 when sugar beets (*Beta vulgaris* L.) were cultivated on the field. Notice that the polygonal pattern was not visible on adjacent fields with a different crop. An aerial photograph of the same field but with a different crop taken 1 yr later did not show the polygonal pattern, demonstrating the ephemeral character of crop marks (Ghysels, 2008). It is our experience that due to their deep rooting system, sugar beets often develop good crop marks. Besides the polygonal pattern, the aerial photograph also shows a former field track, crossing the field from north to southeast. The photograph was georeferenced and color stretched to enhance the contrasts, after which a test area of 0.63 ha was selected and clipped (Arcmap 9.3, ESRI) (Fig. 1b).

Electromagnetic Induction Survey and Data Processing

The test area was surveyed with a Geonics EM38DD sensor which simultaneously measures the EC_a in a horizontal (EC_a–H) and vertical (EC_a–V) dipole mode. With a fixed intercoil spacing of 1 m, each coil pair has its own depth-response curve (McNeill, 1980). When operating at low induction numbers, these response functions are assumed to be independent on soil electrical conductivity (Callegary et al., 2007). The depth of exploration (DOE), defined as the depth where 70% of the response is obtained from the soil volume above this depth, is 0.76 m for EC_a–H and 1.55 m for EC_a–V (Saey et al., 2009). Characteristic for

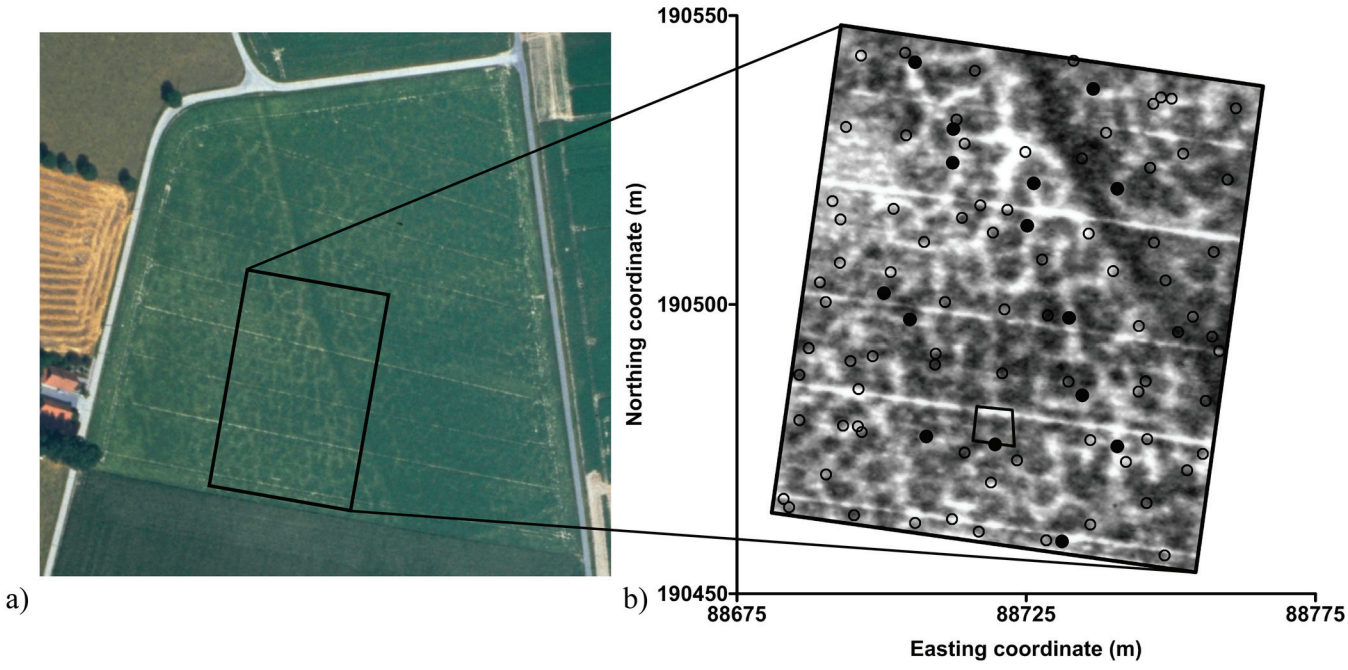

Fig. 1. (a) Aerial photograph taken on 4 Aug. 1996 showing polygonal crop marks and a former field track (north–southeast oriented) with delineation of the test area (large rectangle) (J. Bourgeois, Department of Archeology and Ancient History of Europe, Ghent University, Belgium, Photo: J. Semey) and (b) same aerial photograph after georeferencing, clipping, and color stretching with delineation of the excavated area (small rectangle) and indication of the 94 augering locations (dots). Full dots represent a selection of 15 samples located on the polygonal crop marks. Coordinates are according to the Belgian metric Lambert-72 projection.(Fig. 1 is available in color online.)

EC_a measurements is their strong relationship with soil texture in the absence of salinity (Cockx et al., 2007; Corwin and Lesch, 2005).

The sensor was mounted on a sled pulled by an all terrain vehicle, which drove along parallel lines with an in-between distance of on average 75 cm at a speed from 4 to 6 km h^{-1}. The EC_a was measured with a frequency of 10 Hz and the data were recorded by a field computer. A Trimble AgGPS332, with Omnistar correction, was used to georeference the EC_a measurements with a pass-to-pass accuracy of approximately 0.10 m (Saey et al., 2009). The survey was conducted on 9 Apr. 2010 during dry weather conditions on a bare field with no soil tillage since October 2009.

The EC_a measurements were postcorrected for instrumental drift (Simpson et al., 2009) and standardized to a reference temperature of 25°C (Slavich and Petterson, 1990). A Gaussian low pass filter was applied to the data for noise removal using SGeMS (Remy et al., 2009). Because EC_a values were generally larger at the former field track, we subtracted a moving spatial average (radius = 3 m) from each measurement to highlight the polygon boundaries. Finally, the residuals (ΔEC_a = EC_a – moving average) were interpolated to a grid with a cell size of 0.1 by 0.1 m using ordinary kriging (Surfer 9, Golden Software) (Goovaerts, 1997). Because of the larger data density in the direction of the measurements lines, we used an elliptical search window with a major axis of 2 m perpendicular to the measurement lines and a minor axis of 0.5 m parallel to the measurement lines.

Excavation

In a small part of the field (6 by 6 m) (Fig. 1b) we exposed the polygonal pattern to investigate and characterize the network. An excavator crane systematically removed sediment layers of 0.3 m to a depth of 0.9 m. The horizontal exposure was photographed from a height of about 20 to 30 m using a remotely controlled camera attached to a kite. Afterward, the photograph was georeferenced and color contrast enhanced (Arcmap 9.3, ESRI).

Soil Sampling

To characterize the textural variability of the subsoil, we took 94 subsoil samples within the test area according to a mixed systematic and random scheme. Half of the locations were sampled according to a grid to ensure equal coverage and the other half were randomly located (Fig. 1b). As the casts extended downward from a depth of 0.6 m (see further), samples were taken from the 0.6- to 0.8-m depth interval. The textural fractions were analyzed with the conventional sieve-pipette method.

The results of the texture analyses were classified into two groups by a fuzzy *k*-means algorithm with the FuzMe software (Minasny and McBratney, 2002). The multivariate classification was based on the clay and sand percentage using a Mahalanobis distance matrix and a fuzziness exponent ϕ of 1.6. The determination of ϕ was done following the scheme proposed by McBratney and Moore (1985). Each observation was assigned to the class for which it received the largest fuzzy membership.

RESULTS AND DISCUSSION

Excavated Area

The kite aerial photograph of the 0.9-m deep excavation pit shows a more or less continuous part of a network of polygonal cells with a diameter of about 6 m (Fig. 2). The structures suggest thermal contraction cracking in a permafrost environment, probably during the latter part of the Weichselian (Buylaert et al., 2009). The wedge infillings comprised yellowish brown, structureless sandy sediments with dispersed gravel elements. The pseudomorphs extended down from the base of a 0.6-m thick silty-sandy Quaternary layer and penetrated sandy-clayey host material belonging to the Ypresian stage of the Eocene epoch (55.8–48.6 Ma).

The shape of the ice-wedge casts was irregular with wide (0.3–1.2 m) upper parts. Irregular shapes point to thaw modification as wedge ice melted, though the occurrence of sand in the original wedge filling cannot be excluded. Ghysels and Heyse (2006) described composite-wedge casts at other sites on the same plateau.

Subsoil Textural Variability

The subsoil texture covers four USDA textural classes as shown in Fig. 3. The average soil textural composition corre-

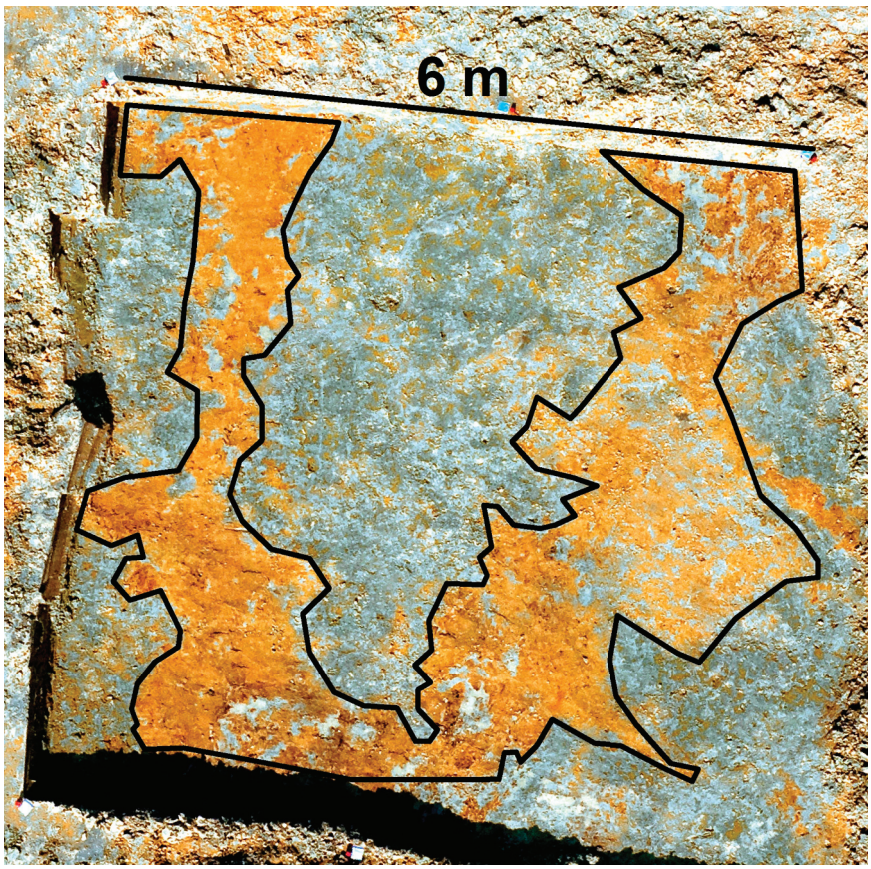

Fig. 2. Kite aerial photograph of the 0.9-m deep excavation pit (6 by 6 m) (enhanced color contrast available online) and indication of the outline of the polygonal network of ice-wedge casts.

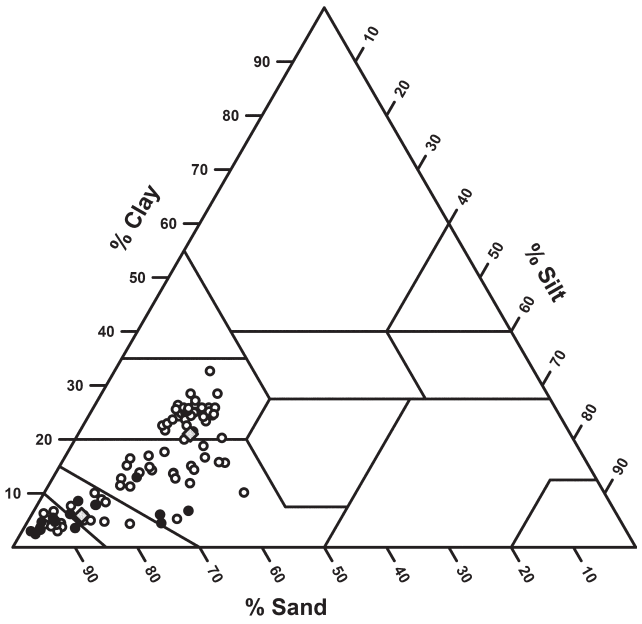

Fig. 3. Results of the 94 texture analyses plotted on the USDA soil texture triangle. The full dots are the selection of 15 samples located on polygonal crop marks on Fig. 1b. The gray diamonds represent the centroids of two classes created by a fuzzy k-means classification.

sponds to a sandy loam texture class, but given the bimodal nature of the textural fractions in this field (see further), the average class is not representative. Table 1 gives the result of the 94 texture analyses of the 0.6 to 0.8 m subsoil samples. The coefficients of variation are 0.19 for the sand fraction, 0.52 for the silt fraction and 0.62 for the clay fraction. This large variability in subsoil texture contrasts strongly with the homogeneous topsoil (not analytically determined but this could clearly be observed in the field by hand feeling) and is responsible for the substantial variation in crop performance.

The fuzzy *k*-means classification resulted in a division of the 94 samples in almost two equal classes (Table 1): class I contained 51 samples with a centroid at 61.3% sand, 17.4% silt, and 21.3% clay (i.e., sandy clay loam) and class II contained 43 samples with a centroid at 85.9% sand, 8.1% silt, and 5.9% clay (i.e., loamy sand) (Fig. 3). A Wilks's lambda test showed that the means of these classes are significantly different ($p < 0.001$).

Based on the aerial photograph we selected 15 sampling locations which were clearly located on a crop mark polygon (Fig. 1b). Since these 15 points were all classified as belonging to class II (Fig. 3), we concluded that class II corresponds to the Quaternary wedge filling, and that the polygonal crop marks visible on the aerial photograph (Fig. 1) represent the network of ice-wedge casts. Hence, class I represents the Tertiary host material.

Image of the Polygonal Network

The average of the 82,770 EC_a–V values was 41.0 mS m^{-1} and of the EC_a–H values it was 32.3 mS m^{-1}. This indicates that the deeper soil layers have an overall higher EC_a. The pearson correlation coefficient between the EC_a–V and EC_a–H values was 0.88 and the pattern shown by both maps was very similar.

Table 1. Results of the texture analyses of the subsoil (0.6–0.8 m) samples taken within the test area.

Textural fractions	Average	Minimum	Maximum	Variance
	%			$\%^2$
	All samples (n = 94)			
sand	72.6	52.0	95.6	191.5
silt	13.1	1.4	32.0	46.5
clay	14.3	2.5	32.7	77.8
Class I (n = 51)				
sand	61.3	52.0	74.1	28.0
silt	17.4	10.6	32.0	16.6
clay	21.3	10.2	32.7	28.2
Class II (n = 43)				
sand	85.9	68.4	95.6	53.8
silt	8.1	1.4	24.9	35.8
clay	5.9	2.5	13.0	7.2

However, the ΔEC_a–H map showed sharper contrasts revealing the polygons in more detail. So regardless of their smaller DOE, measurements taken in the horizontal dipole mode proved more appropriate to map the ice-wedge casts in the subsoil. A possible explanation is that the EC_a–V measurements received a larger response from the Tertiary material underlying the ice-wedge casts, which masked the influence of their sandy infillings. Despite our experience (Cockx et al., 2006), a combination of both signals did not result in an improvement. Therefore, we continued with the ΔEC_a–H map shown in Fig. 4a and further indicated as ΔEC_a map. Similar to the classification of the subsoil samples, a *k*-means classification of the ΔEC_a map resulted in two classes of approximately equal size meaning that both subsoil textures occur with about the same frequency.

The ΔEC_a map (Fig. 4a) images the polygonal network of ice-wedge casts clearly due to the lower EC of the wedge filling, caused by its lower clay content. In general, positive ΔEC_a values correspond to the host material, whereas negative ΔEC_a values correspond to the wedge filling. For comparative reasons, Fig. 4b shows the georeferenced aerial photograph. Although one image represents the variability in soil electrical conductivity and the other one in crop color, it can be observed that both are very similar. However, measuring EC_a is much less dependent from external conditions than observing crop marks, asking for a particular combination of crop and climatic conditions. The five parallel white horizontal lines on the aerial photograph are due to a nonuniform sowing density.

Verification

For each of the 94 sampled locations the ΔEC_a was extracted from the ΔEC_a map to investigate the relationship between soil texture and ΔEC_a. The pearson correlation coefficient between ΔEC_a and the subsoil textural fractions was -0.68 for sand, 0.46 for silt, and 0.71 for clay. So it is clear that ΔEC_a is a proxy for the subsoil clay and sand content. Figure 5 illustrates these relationships and confirms the existence of two distinctly different subsoil classes.

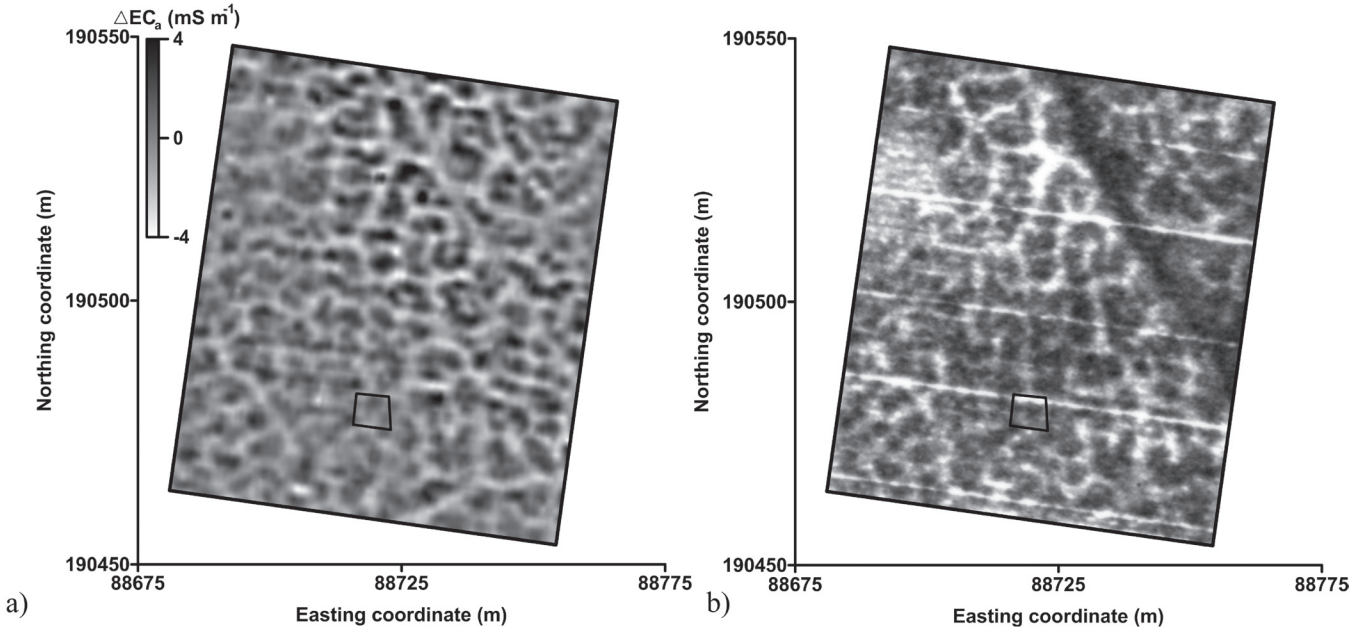

Fig. 4. (a) ΔEC$_a$ (mS m^{-1}) map and (b) georeferenced aerial photograph taken on 4 Aug. 1996 with delineation of the excavated area (small rectangle).

Figure 6 shows a detail of the ΔEC$_a$ map around the excavated area with indication of the boundary of the exposed polygon (Fig. 2). The differences between the wedge filling and the host material are clearly visible on the ΔEC$_a$ map confirming the direct relationship between the processed EC$_a$ measurements and the presence of ice-wedge casts in the subsoil of this area.

CONCLUSIONS

A textural difference between host material and wedge filling is the key for successfully mapping polygonal networks of ice-wedge casts with EMI sensors. In contrast to being dependent on occasional aerial photographs of polygonal crop marks, the use of mobile EMI sensors offers a more generally applicable method to map ice-wedge pseudomorphs, even when these are covered by a topsoil layer of 0.6 m. This noninvasive, fast method offers detailed exhaustive information about the morphology of the cryogenic features.

Our study showed that the presence of ice-wedge casts in the subsoil can be responsible for a highly heterogeneous subsoil texture. About half of the test area has a sandy clay loam subsoil texture, as indicated on the 1/20,000 soil map of Belgium. The other half represents the ice-wedges which contain considerably more sand and consequently less clay. Because the presence of both textures is spatially structured and can be mapped, this situation can be considered as a challenge for managing the within field variability to optimize crop yield, that is, precision agriculture.

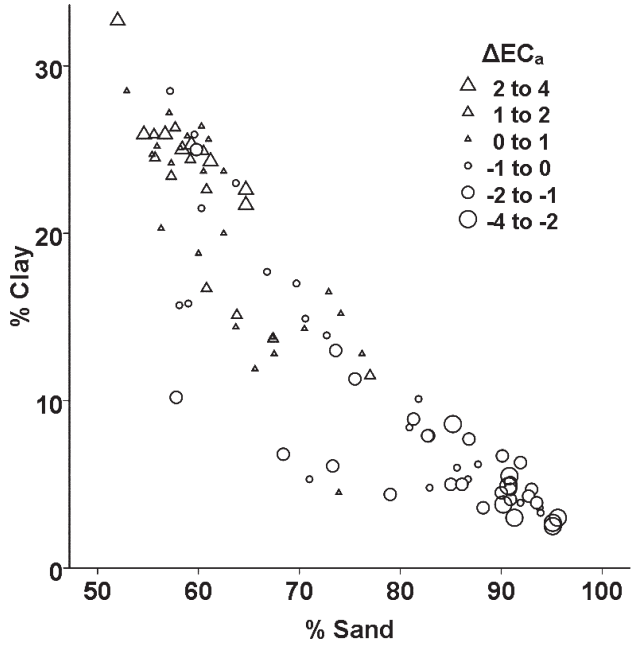

Fig. 5. Subsoil (0.6–0.8 m) clay and sand content in relation to ΔEC$_a$: the size and shape of the symbols correspond to the ΔEC$_a$ value measured at the same location.

ACKNOWLEDGMENTS

This research was supported by the Fund for Scientific Research-Flanders (FWO-Vlaanderen). The authors thank the farmer for granting access to his field and Valentijn Van Parys for his help with the field work.

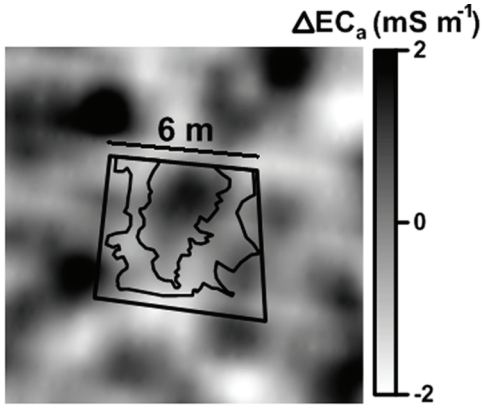

Fig. 6. Detail of the ΔEC$_a$ map with indication of the excavated area and the observed polygon outline (as shown in Fig. 2).

REFERENCES

Buylaert, J.P., G. Ghysels, A.S. Murray, K.J. Thomsen, D. Vandenberghe, F. De Corte, I. Heyse, and P. Van den Haute. 2009. Optical dating of relict sand wedges and composite-wedge pseudomorphs in Flanders, Belgium. Boreas 38:160–175. doi:10.1111/j.1502-3885.2008.00037.x

Callegary, J.B., T.P.A. Ferre, and R.W. Groom. 2007. Vertical spatial sensitivity and exploration depth of low-induction-number electromagnetic-induction instruments. Vadose Zone J. 6:158–167.

Cockx, L., G. Ghysels, M. Van Meirvenne, and I. Heyse. 2006. Prospecting ice-wedge pseudomorphs and their polygonal network using the electromagnetic induction sensor EM38DD. Permafrost Periglac. 17:163–168. doi:10.1002/ppp.546

Cockx, L., M. Van Meirvenne, and B. De Vos. 2007. Using the EM38DD soil sensor to delineate clay lenses in a sandy forest soil. Soil Sci. Soc. Am. J. 71:1314–1322. doi:10.2136/sssaj2006.0323

Corwin, D.L., and S.M. Lesch. 2005. Characterizing soil spatial variability with apparent electrical conductivity: I. Survey protocols. Comput. Electron. Agric. 46:103–133. doi:10.1016/j.compag.2004.11.002

Dansart, A.M., J.M. Bahr, and J.W. Atig. 1999. Using ground-penetrating radar to map fossil permafrost wedges that are preferential flow pahts for leaching to groundwater. GSA Abstracts with Programs 31:A-76.

Doolittle, J., and F. Nelson. 2009. Characterising relict cryogenic macrostructures in mid-latitude areas of the USA with three-dimensional ground-penetrating rRadar. Permafrost Periglac. 20:257–268. doi:10.1002/ppp.644

Dutilleul, P., T.W. Haltigin, and W.H. Pollard. 2009. Analysis of polygonal terrain landforms on Earth and Mars through spatial point patterns. Environmetrics 20:206–220. doi:10.1002/env.924

French, H.M. 2007. The periglacial environment. 3rd ed. John Wiley & Sons, Chichester.

Ghysels, G. 2008. Bijdrage tot de studie van de kenmerken, de genese en de datering van periglaciale polygonale wigstructuren in België. Ph.D. diss. Ghent Univ., Ghent.

Ghysels, G., and I. Heyse. 2006. Composite-wedge pseudomorphs in Flanders, Belgium. Permafrost Periglac. 17:145–161. doi:10.1002/ppp.552

Goovaerts, P. 1997. Geostatistics for natural resources evaluation. Oxford Univ. Press, New York.

Harry, D.G., and J.S. Gozdzik. 1988. Ice wedges: Growth, thaw transformation, and palaeoenvironmental significance. J. Quaternary Sci. 3:39–55. doi:10.1002/jqs.3390030107

Kolstrup, E. 1986. Reappraisal of the upper Weichselian periglacial environment form Danish frost wedge casts. Palaeogeogr. Palaeocl. 56:237–249. doi:10.1016/0031-0182(86)90096-9

Lusch, D.P., K.E. Stanley, R.J. Schaetzl, A.D. Kendall, R.L. Van Dam, A. Nielsen, B.E. Blumer, T.C. Hobbs, J.K. Archer, J.L.F. Holmstadt, and C.L. May. 2009. Characterization and mapping of patterned ground in the Saginaw Lowlands, Michigan: Possible evidence for late-Wisconsin permafrost. Ann. Assoc. Am. Geogr. 99:445–466. doi:10.1080/00045600902931629

Mackay, J.R., and C.R. Burn. 2002. The first 20 years (1978–1979 to 1998–1999) of ice-wedge growth at Illisarvik experimental drained lake site, western Arctic coast, Canada. Can. J. Earth Sci. 39:95–111. doi:10.1139/e01-048

McBratney, A.B., and A.W. Moore. 1985. Application of fuzzy sets to climatic classification. Agric. For. Meteorol. 35:165–185. doi:10.1016/0168-1923(85)90082-6

McNeill, J.D. 1980. Electromagnetic terrain conductivity measurement at low induction numbers. Geonics Ltd., Mississauga, ON.

Minasny, B., and A.B. McBratney. 2002. FuzMe version 3. Australian Centre for Precision Agric., The Univ. of Sidney, NSW.

Morgan, A.V.M. 1971. Engineering problems caused by fossil permafrost features in the English Midlands. Q. J. Eng. Geol. Hydroge. 4:111–114. doi:10.1144/GSL.QJEG.1971.004.02.02

Murton, J.B., and H.M. French. 1993. Thaw modification of frost-fissure wedges, Richards Island, Pleistocene Mackenzie Delta, western Arctic Canada. J. Quaternary Sci. 8:185–196. doi:10.1002/jqs.3390080302

Plug, L.J., and B.T. Werner. 2002. Nonlinear dynamics of ice-wedge networks and resulting sensitivity to severe cooling events. Nature (London) 417:929–933. doi:10.1038/nature00796

Plug, L.J., and B.T. Werner. 2008. Modelling of ice-wedge networks. Permafrost Periglac. 19:63–69. doi:10.1002/ppp.604

Remy, N., A. Boucher, and J. Wu. 2009. Applied geostatistics with SGeMS: A user's guide. Cambridge Univ. Press, New York.

Romanovskij, N.N. 1973. Regularities in formation of frost-fissure polygons and development of frost-fissure polygons. Biuletyn Peryglacjalny 23:237–277.

Saey, T., D. Simpson, H. Vermeersch, L. Cockx, and M. Van Meirvenne. 2009. Comparing the EM38DD and DUALEM-21S Sensors for depth-to-clay mapping. Soil Sci. Soc. Am. J. 73:7–12. doi:10.2136/sssaj2008.0079

Simpson, D., M. Van Meirvenne, T. Saey, H. Vermeersch, J. Bourgeois, A. Lehouck, L. Cockx, and U.W.A. Vitharana. 2009. Evaluating the multiple coil configurations of the EM38DD and DUALEM-21S sensors to detect archaeological anomalies. Archaeol. Prospect. 16:91–102. doi:10.1002/arp.349

Slavich, P.G., and G.H. Petterson. 1990. Estimating average rootzone salinity for electromagnetic (EM-38) measurements. Aust. J. Soil Res. 31:2401–2409.

Vandenberghe, J., and A. Pissart. 1993. Permafrost changes in Europe during the Last Glacial. Permafrost Periglac. 4:121–135. doi:10.1002/ppp.3430040205

Walters, J.C. 1994. Ice-wedge casts and relict polygonal patterned ground in North-East Iowa, USA. Permafrost Periglac. 5:269–281. doi:10.1002/ppp.3430050406